




## South African dust contribution to the high southern latitudes and East Antarctica during interglacial stages

Stefania Gili <sup>1,2✉</sup>, Aubry Vanderstraeten<sup>1,3</sup>, Amélie Chaput<sup>4</sup>, James King <sup>4</sup>, Diego M. Gaiero<sup>5</sup>, Barbara Delmonte<sup>6</sup>, Paul Vallenga<sup>7</sup>, Paola Formenti<sup>8</sup>, Claudia Di Biagio<sup>8</sup>, Mathieu Cazanau<sup>8</sup>, Edouard Pangui<sup>8</sup>, Jean-François Doussin <sup>8</sup> & Nadine Mattielli<sup>1</sup>

Mineral dust is a natural tracer of atmospheric composition and climate variability. Yet, there is still much to be known about the Southern Hemisphere dust cycle. Major efforts have attempted to solve the puzzle of the origin of the potential source areas contributing dust to the Southern Ocean and East Antarctica. Here we present a comprehensive geochemical characterization of a source area, whose role as a dust supplier to high latitude environments has significantly been underestimated. Sediments collected within the major dust-producing areas along the Namibian coast in Southern Africa (Kuseb, Omaruru and Huab river catchments and the Namib Sand Sea region), were analyzed for radiogenic isotope ratios and rare earth element concentrations. We find that during warm periods, the Southern African dust signature can be found in archives of the Southern Hemisphere, especially in the Atlantic sector of the Southern Ocean and peripheral areas of the East Antarctic plateau.

<sup>1</sup>Laboratoire G-Time, Département Géosciences, Environnement et Société (DGES), Université Libre de Bruxelles (ULB), B-1050 Brussels, Belgium.

<sup>2</sup>Department of Geosciences, Princeton University, Princeton, NJ, USA. <sup>3</sup>Univ. Littoral Côte d'Opale, CNRS, Univ. Lille, UMR 8187 - LOG - Laboratoire d'Océanologie et de Géosciences, F-62930 Wimereux, France. <sup>4</sup>Laboratoire d'Érosion Éolienne, Département de Géographie, Université de Montréal, Montréal, Canada. <sup>5</sup>CICTERRA/CONICET, Universidad Nacional de Córdoba, Córdoba, Argentina. <sup>6</sup>Department of Environmental and Earth Sciences, University of Milano-Bicocca, Milan, Italy. <sup>7</sup>UWA Oceans Institute, University of Western Australia, Perth, Australia. <sup>8</sup>Université Paris Cité and Univ Paris Est

Creteil, CNRS, LISA, F-75013 Paris, France. ✉email: [sgili@princeton.edu](mailto:sgili@princeton.edu)

Mineral dust is considered a sensitive natural tracer of modern and past environmental conditions and a paleoclimatic proxy that reflects the variations in the atmospheric circulation during different climatic periods and their transitions. The type and intensity of dust emissions are a consequence of different conditions at the source (sediment supply and availability) and aeolian processes (deflation, transport, deposition)<sup>1</sup>. Once dust is emitted into the atmosphere, it remains in suspension until physical and chemical conditions favor its deposition. The deposited dust is archived in different proxy records either, over the oceans or onto continental landmasses within ice cores, deep-sea sediments, loess, peat bogs, etc. For the Southern Hemisphere, reconstructions of dust buried in Antarctic ice cores are considered an excellent proxy for the paleo-record of wind intensity and circulation. In this regard, these records indicated that dust fluxes were up to ~25 times higher during glacial periods due to dust production strengthening at their source areas, compared to warmer periods when dust concentrations were extremely low<sup>2</sup>.

The term Potential Source Areas (PSAs) denotes either a primary source of mineral dust, derived directly from the physical and/or the chemical weathering of the parent material or a secondary source for dust, where airborne particles have already been subjected to a phase of aeolian and/or fluvial transport<sup>3</sup>. For the Southern Hemisphere, Southern South America (SSA), Australia (AUS), New Zealand (NZ), Southern Africa (SAF), and the Antarctic Dry Valleys have all been identified as PSAs. The first study to trace the dust origin in Antarctica identified SSA as the source area from which dust from the Last Glacial Maximum (LGM) section of the Dome C ice core was derived<sup>4</sup>. In agreement with the Sr-Nd isotope data presented in that study, all the studies since then have demonstrated that the main dust contributor to the Southern Ocean (SO) and East Antarctica (EA) during glacial (MIS2-MIS20) and interglacial periods was SSA, mainly Patagonia<sup>3,5-10</sup>. Despite the agreement on the dominance of a Patagonian dust origin during glacial periods, there is currently a debate regarding the Holocene dust PSAs with the following scenarios of dust provenance proposed: (i) a weakened Patagonian source complemented by a lower latitude source region (Southern Central West Argentina, SCWA<sup>7,10,11</sup>); (ii) a Puna–Altiplano dust source transported via the southern tropical jet stream<sup>7,9,10,12</sup> and, (iii) a general contribution from Southern South America plus a secondary input from AUS<sup>13-17</sup> or NZ<sup>17</sup>. Some of these geochemical and mineralogical interpretations were partially supported by Atmospheric General Circulation Models (AGCMs), suggesting that while SSA dust dominates deposition over the Atlantic Southern Ocean and East Antarctica, AUS modern dust prevails over the Pacific SO and towards the western coastal regions of Antarctica<sup>18-20</sup>. Additionally, two important recent studies reviewed and evaluated the role of AUS as a dust source during modern and Late Quaternary times showing that Australian dust likely reached certain sectors of Antarctica, such as Taldice and Taylor Glacier, predominantly during interglacials periods<sup>21,22</sup>. For NZ, back-trajectory modeling showed that the transportation of aeolian material from this region to the southern high latitudes is possible<sup>23</sup>. However, a recent study carried out on sediments from the major present-day dust and sediment producing regions of the South Island in NZ, has indicated this area was not a significant dust supplier to EA<sup>24</sup>.

AGCMs have shown that after SSA and AUS, Southern Africa is the third main dust supplier in the Southern Hemisphere with dust depositions mainly taking place in the South Atlantic and Indian Oceans<sup>18</sup>. Even though this region is a significant dust emission source, little is still known about it being a Potential source area as the geochemical and modeling data available for this region is extremely sparse. Thus, it is questionable if the role

of SAF as a dust contributor to the SO and EA has plausibly been underestimated. For many years, only the Makgadikgadi Pan in Botswana and the Etosha Pan in Namibia were recognized as persistent dust sources in SAF<sup>18,25-27</sup>, neglecting the coastal Namibian sources. In fact, it was only until recently that the Namib Desert coast has been identified as one of the largest sources of dust in Southern Africa<sup>28,29</sup>. Using remote sensing satellite images, these authors have found that along the southwestern coast of SAF, the Kuiseb, Omaruru, and Huab Rivers beds are the three main areas of greatest dust emission located on recently deposited fluvial surfaces. Revisiting the literature, it became apparent that while most of the studies have been focused on the detailed study of SSA, AUS, and most recently NZ dust sources<sup>9,10,15,21,22,24</sup>, other PSAs, such as SAF, have been overlooked. Thus, there arises a compelling need for more extended geochemical studies to fill the current gap in understanding the past and present long-range transportation of mineral dust particles to the high-latitude environments.

Responding to this need, this study aims to investigate the role of SAF as a PSA and provides the first comprehensive north-to-south geochemical characterization of riverbed sediments collected along the major dust-producing river systems in the Namib desert (Huab, Omaruru, Kuiseb and the Namibia Sand Sea) (Fig. 1a). It is nevertheless noteworthy that many of these river catchments have been (and still are), subject to extreme anthropogenic activities, mainly because the alluvial deposits of the rivers hold the groundwater that supports urban and industrial development in the region<sup>30</sup>. Such activities can substantially modify these hydrographic systems affecting the natural dust emission sources and increasing, as a consequence, the dust production in certain areas (see more details in Supplementary Note 1).

The Namib desert extends N-S for approximately 2000 km along the western coast of southern Africa between the Kunene and Orange Rivers<sup>31</sup>. This massive and arid region of SAF, consists of a complex system of different geomorphological structures (deltas, ephemeral rivers, pan complexes, dune fields, gravel plains) and each of these structures comprises several landforms (floodplain terraces, river channels, nebkhas, basins, margins of playas and sabkhas, stone pavement) that have proven to be accountable for sediment entrainment and wind erosion<sup>29,32</sup>. The eastern border for the Namib desert is delimited by the Great Escarpment (~2000 msal) running parallel to the coast and 100–150 km inland. Traversing the escarpment, between the Kunene and the Orange Rivers, twelve aligned ephemeral river valleys extend sub-parallel east-west along the Atlantic Coast<sup>30</sup>. The rainfall in the headwaters of these river catchments (250–350 mm/year) generates floods that can last a few days flowing through the Namib Desert eastward towards the coast. However, because that rainfall becomes insignificant towards coastal areas (<25 mm/year), the limited floods only reach the ocean occasionally<sup>33</sup>. Thus, the water that dissipates due to infiltration and evaporation along with a decrease in vegetation, makes the deposited sediments at the terminal stages of the river valley channels available for aeolian entrainment and transport. In addition, the presence of erosion agents, such as salting sands from the Namib Sand Sea region, sediment mineralogy and grain size, vegetation roughness, and soil moisture are all parameters responsible for controlling the dust emission rate along the SAF coast<sup>34</sup>. Anthropogenic disturbances of certain dust production areas are also worth mentioning. Especially the hydrological systems of Omaruru and Kuiseb, where the increased demand for water extraction and diversion in combination with population growth has played a role in altering some of the main landforms<sup>29,35</sup>. The arid and stable climate of the Namibian coast is produced by the quasi-stationary

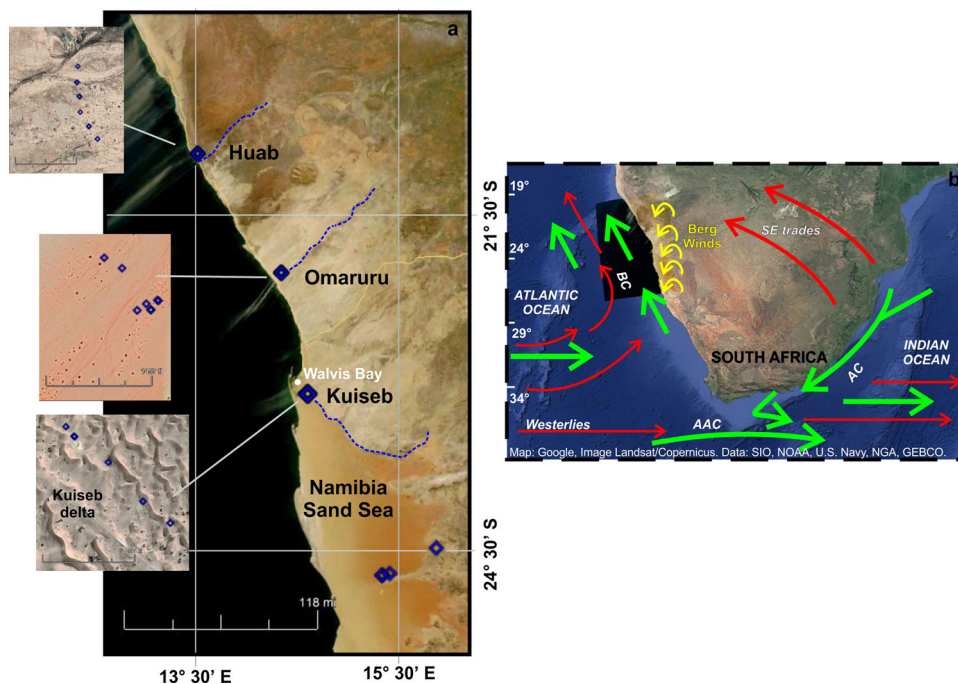


**Fig. 1** Geographical and climatological characterization of Southern Africa Potential dust source areas. **a** satellite image of dust plumes originated off the coast of Namibia captured in May 2013 by The Moderate Resolution Imaging Spectroradiometer (MODIS) on NASA's Terra satellite showing the study areas of Huab, Omaruru, Kuiseb and the Namibia Sand Sea. The hydrographic Huab, Omaruru and Kuiseb systems are indicated by the blue lines. **b** map of southwestern Africa showing the major features of the regional climate system. Main oceanic currents are indicated in bold green arrows and atmospheric circulations in red (south easterly trade and westerlies winds) and yellow (Berg winds). BC: Benguela Current; ACC: Antarctic Circumpolar Current; AC: Agulhas Current. The map in Fig. b was built using Google Earth Pro, Image Landsat/Copernicus; Data: SIO, NOAA, U.S. Navy, NGA, GEBCO, 13 December 2015.

subtropical South Atlantic High Pressure (anticyclone) system and the cold northward-flowing Benguela current<sup>36</sup> (Fig. 1b). This upwelling system is wind-driven by the regional alongshore Southeast trade-winds (Fig. 1b) and is recognized for being a region with the highest rates of primary production in the ocean where dust with high nutrient content deflated from the continent is discharged offshore fertilizing the ocean waters<sup>37</sup>. Although minimum annual variations in wind intensities occur, the Benguela upwelling system is often separated into three zones; north, central, and south<sup>38</sup>. The north and south Benguela upwelling zones are respectively bounded by the Angola and Agulhas Currents. The central zone presents the least fluctuating regime and is the most relevant zone for our research as it lies contiguous to the main dust source region investigated here between 22° and 28°S. Another important atmospheric agent of aerosol transport and deposition off the Namibian coast are the so-called Berg winds (Fig. 1b). These are katabatic winds, generally blowing from the east and northeast, supplying large amounts of aeolian dust into the SE Atlantic Ocean due to their high velocities and subsidence offshore<sup>39</sup>. Common from April to August, associated with high daily evaporation rates and low monthly fog–water precipitation values, the Berg winds are locally intensified by topographic features such as river valleys and are shown to be responsible for >60% of the offshore sediment transport with dust plumes extending  $\geq 100$  km into the Southern Ocean. In addition, with an estimated annual dust input of 4.4 tons into the South Atlantic Ocean, these Berg winds are in charge of supplying nutrients to the highly fertile Benguela upwelling system<sup>28,40</sup>.

In this work, we combine rare earth elements (REE) concentrations and the Sr-Nd-Pb isotope compositions to evaluate the contribution of Southern African dust to the high latitude environments of the Southern Hemisphere. This is, to the high

elevation sites of East Antarctica with a special focus on the coastal sites and the Atlantic sector of the Southern Ocean. We compare the geochemical signature of bulk and resuspended aerosol fractions from SAF, with the dust fingerprint reported for Antarctic ice cores (Vostok and EDC) during glacial (MIS2–MIS20) and interglacial periods (Holocene and MIS 5.5) as well as present-day dust from Berkner Island<sup>41</sup>. In addition, we also include a re-analysis of the isotopic composition of SAF samples previously reported in<sup>3,8</sup>. The results presented will demonstrate that the SAF dust signature can be an important additional end-member in explaining the dust fingerprint found in the South Atlantic Ocean and coastal regions of East Antarctica.

## Results

**Geochemical characterization of Southern Africa potential source areas.** The complete REE concentrations and Sr-Nd-Pb isotopic composition database of the samples presented in this study are presented in Supplementary Data 1. The Southern Africa PSAs signature of the windblown samples presented in this study reflect the compositional variability of the locally outcropping rocks and sediments: a chemical and isotopic fingerprint that is the result of the mixing between the Damara Orogenic system including 2.0–1.2 Ga gneissic basement overlaid by Neoproterozoic to Paleozoic metasediments intruded by 840–460 Ma granitoid plutons, and the Orange River sediments<sup>42,43</sup> (see more details in Supplementary Note 1 and Supplementary Fig. 1).

In Fig. 2, REE patterns for the Southern Africa PSAs normalized to the upper crust (UCC<sup>44</sup>) are plotted. This figure indicates that no significant difference in the REE composition prevails among all four areas characterized in this study and a regional differentiation is difficult. In general, samples show flat REE patterns with a minor decrease in the heavy REE abundances

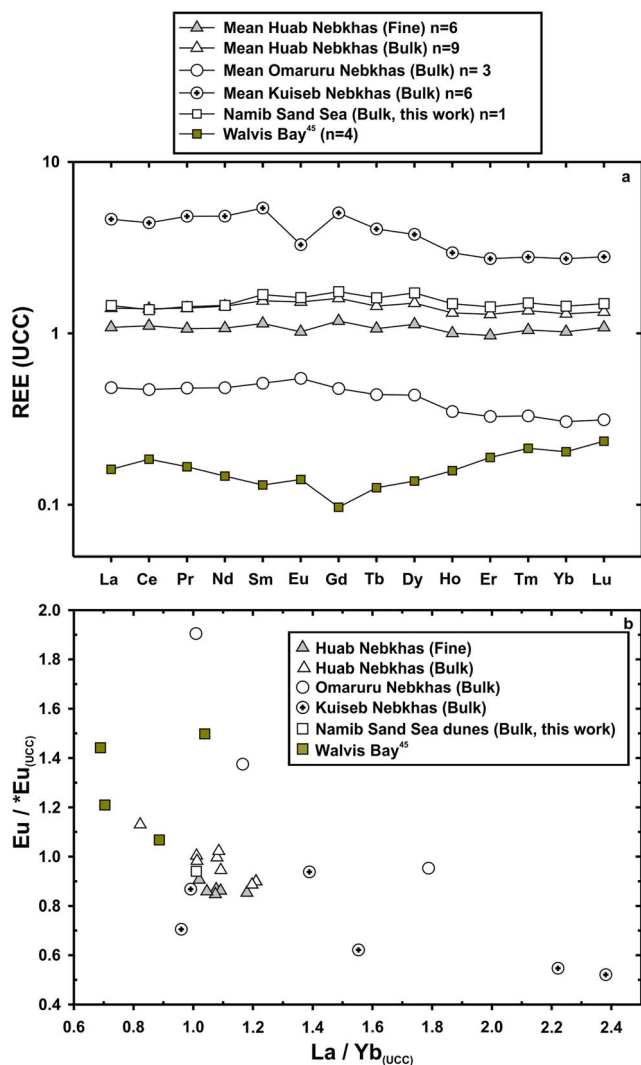


**Fig. 2 Rare Earth Elements (REE) data of surface sediments representing the Potential source areas of Southern Africa.** **a** Mean REE patterns. **b** Relationships between  $Eu / *Eu$  and  $La / Yb_{(UCC)}$ . REE data has been normalized to upper continental crust<sup>44</sup>. Errors bars are smaller than symbols.

(Fig. 2a). Note that for the Omaruru catchment only the REE data for three out seven samples are available. Both the bulk and the fine fractions from Huab and Kuiseb exhibit  $Eu / Eu^* < 1$ , with Omaruru displaying slightly higher values (Fig. 2b) for this ratio. For the Namib Sand Sea region, only one data point for a bulk sample is available in terms of REE and its composition is similar to the Huab area. The Eu anomaly ( $Eu / Eu^*$ ) was calculated with the equation  $Eu / Eu^* = \frac{1}{4} [Eu] / (([Sm] + [Gd]) / 2)$ . Figure 2b also shows that the REE composition of the bulk and the fine fractions from the Huab area are similar, suggesting bulk samples are representative of the fine particles and that Southern Africa REE signature is independent of the grain-size fraction of sediments. For comparison purposes, soil samples from the Walvis Bay in Namibia have also been included (Fig. 2a, b), whose source has been attributed to the local dust blown from the nearby Namibia Sea Sand<sup>45</sup>.

Compared to REE data, the Huab, Omaruru, Kuiseb and Namib Sea Sand samples can be better discriminated based on their isotopic compositions (Fig. 3). Lead isotope compositions span within a relatively large range of values:  $^{206}Pb / ^{207}Pb$ : 1.15–1.28,  $^{208}Pb / ^{207}Pb$ : 2.43–2.62 defining variable Pb isotope

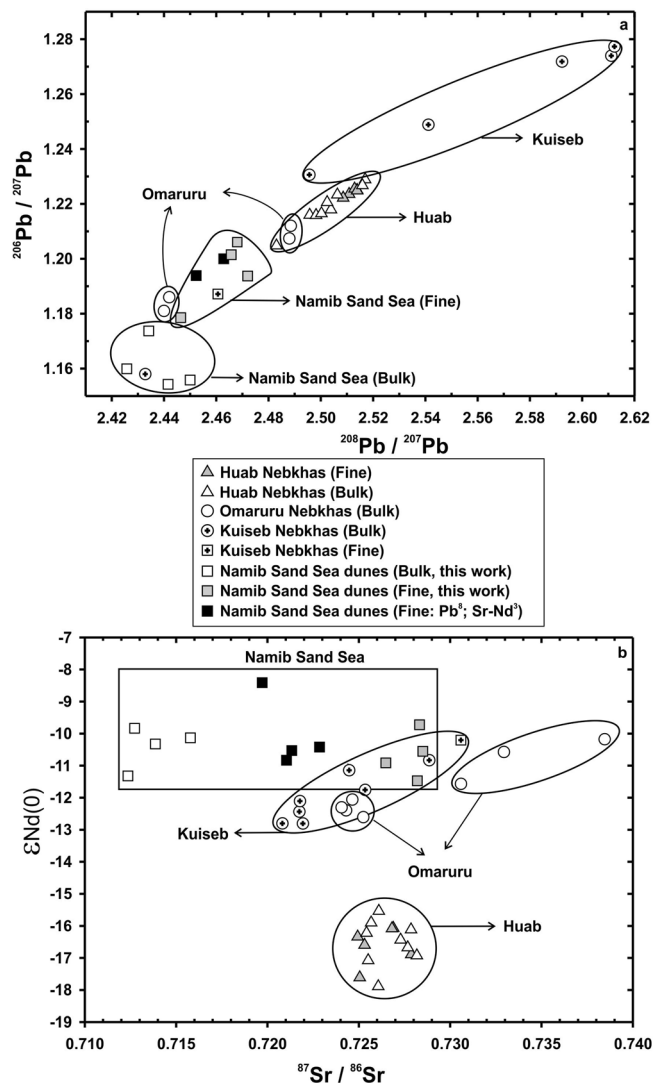


**Fig. 3 Sr-Nd-Pb isotopic compositions of Southern Africa sediments.** **a**  $^{208}Pb / ^{207}Pb$  vs.  $^{206}Pb / ^{207}Pb$ . **b**  $^{87}Sr / ^{86}Sr$  vs.  $\epsilon Nd(0)$ . Grain size effects on Sr-Nd-Pb isotopic compositions for the Huab and Namib Sand Sea are also shown and indicated by symbols in gray (fine) and open symbol (bulk).

fields (Fig. 3a). For the Huab valley, the nebkhass in both the bulk and fine fractions display intermediate lead values ( $^{206}Pb / ^{207}Pb$ : 1.205–1.228,  $^{208}Pb / ^{207}Pb$ : 2.482–2.518). This is, between the bulk fraction of the sand dunes from Kuiseb and the Namib Sand Sea regions which represent the highest and lowest (respectively) end-members in terms of Pb isotopic compositions. In this sense, the Kuiseb related samples have a more Th-rich signature ( $^{206}Pb / ^{207}Pb$ : 1.23–1.277,  $^{208}Pb / ^{207}Pb$ : 2.495–2.612) indicating derivation from sources with higher Th/U ratios. Contrarily, the Namib Sand Sea area shows comparatively the most unradiogenic Pb isotopic values ( $^{206}Pb / ^{207}Pb$ : 1.159–1.206,  $^{208}Pb / ^{207}Pb$ : 2.425–2.468), with a clear distinction between the bulk and the fine fractions. Interestingly, nebkhass samples associated with the Omaruru valley define two isotopic subfields: one overlapping with Huab and a second field with less radiogenic isotopic ratios ( $^{206}Pb / ^{207}Pb$ : 1.181–1.212,  $^{208}Pb / ^{207}Pb$ : 2.439–2.488) showing a similar fingerprint to the fine fraction of the Namib Sea Sand (Fig. 3a). We also observe a Pb isotope offset between our bulk and fine fraction for one sample from the Kuiseb catchment and the previously published values on the same sample<sup>8</sup>. Our Pb



values for that sample are more similar to the Namib Sand Sea dunes (Fig. 3a).

As a whole, the Sr–Nd isotopic ratios from SAF samples measured in this study in both the bulk and fine fractions (Fig. 3b) exhibit two main groups, indicating plausible dust provenance from different source end-members coherent with the geological history of this part of the continent. The isotopic variability in the bulk fraction for sediment samples derived from the Omaruru and the Kuiseb river systems is large ( $^{87}\text{Sr}/^{86}\text{Sr} = 0.7208\text{--}0.7384$  and  $\epsilon\text{Nd}(0) = -12.80$  to  $-10.17$ ). In contrast, the bulk and fine fractions of the Namib Sand Sea dune samples depict an even broader range of isotopic values:  $^{87}\text{Sr}/^{86}\text{Sr} = 0.7128\text{--}0.7305$  and  $\epsilon\text{Nd}(0) = -10.39$  to  $-9.84$ , reflecting provenance from the granitoid intrusions of the Damara belt<sup>46</sup>. The nebkhas from the Huab catchment, which drains the Paleoproterozoic basement of the Kaoko belt<sup>43</sup>, display a narrower range of isotopic values for both the bulk and fine fractions:  $^{87}\text{Sr}/^{86}\text{Sr} = 0.725\text{--}0.728$  and  $\epsilon\text{Nd}(0) = -18$  to  $-15$ . We also observe a Nd isotopic trend with values becoming progressively less radiogenic from north to south. This is, the Huab region (in the north of the Namib coastline), exhibits the less radiogenic Nd composition with  $\epsilon\text{Nd}(0)$  between  $-18$  and  $-15$ , continuing towards the Omaruru and Kuiseb valleys with intermediate Nd compositions before reaching the southernmost location of the Namib Sand Sea region which exhibits  $\epsilon\text{Nd}$  values between  $-10.5$  and  $-8$ . We also observe a Sr isotopic offset between our fine fraction samples from the Namib Sand Sea dunes and the previously published values on the same samples<sup>3</sup> with our dataset showing higher  $^{87}\text{Sr}/^{86}\text{Sr}$  values ( $>0.725$ , Fig. 3b).

**Grain-Size isotopic fractionation.** Attributable to different mineral contributions, mainly clays and feldspars, that are ultimately controlled by mineral sorting processes<sup>47</sup>, it is observed that the fine-grained fractions generally show a more-radiogenic signature compared to the bulk of the same samples. In the present study, the set of samples from the Huab ( $n = 6$ ), Kuiseb ( $n = 1$ ), and the Namib Sand Sea ( $n = 4$ ) regions analyzed in the bulk and the fine fractions, conforms to the longstanding observation that there are statistically significant differences in  $^{87}\text{Sr}/^{86}\text{Sr}$ , but much less so for  $\epsilon\text{Nd}(0)$  and Pb isotopic values (Fig. 3a, b). While the dunes from Kuiseb and the Namib Sand Sea show the highest Sr isotopic differences ( $\Delta ^{87}\text{Sr}/^{86}\text{Sr} \sim 0.012$  units), the variability in nebkhas from the Huab region is limited to only  $\sim 0.002$  units (Fig. 3b). Furthermore, for the three areas the mean difference between  $\epsilon\text{Nd}(0)$  values for the fine and bulk fractions is  $<1\epsilon$  units and not significant. For Lead, these differences are also small ( $\Delta ^{206}\text{Pb}/^{207}\text{Pb}$  and  $^{208}\text{Pb}/^{204}\text{Pb} \sim 0.022$  units for Kuiseb, and Namib Sand Sea samples and, even smaller  $\Delta$  for the Huab samples:  $\sim 0.01$  units) meaning that the sorting by size, although not a zero effect, does not play a significant role that could complicate attempts to relate the Pb isotope data in remote locations to PSAs. Overall, our results agree with the observed small differences between clay and silt for grain-size fractions in river sediments<sup>48</sup>. The new data presented here for the finer fraction in dunes samples from the Namibia Sand Sea, agrees with the previous Pb isotopic ratios ( $n = 2$ ) reported for the same region<sup>8</sup>. As mentioned above, the strontium isotope ratios previously presented for this area<sup>3</sup>, are slightly less radiogenic in  $^{87}\text{Sr}/^{86}\text{Sr}$  compared with the new values obtained here for the same samples (Fig. 3b). Despite the disparity, this does not affect our interpretations; any difference in the Sr isotopic data between the bulk and the fine grain-size fractions of sediments is small compared to the variability of the whole Southern Africa region, reinforcing the hypothesis that the isotopic signatures can be used to fingerprint provenance.

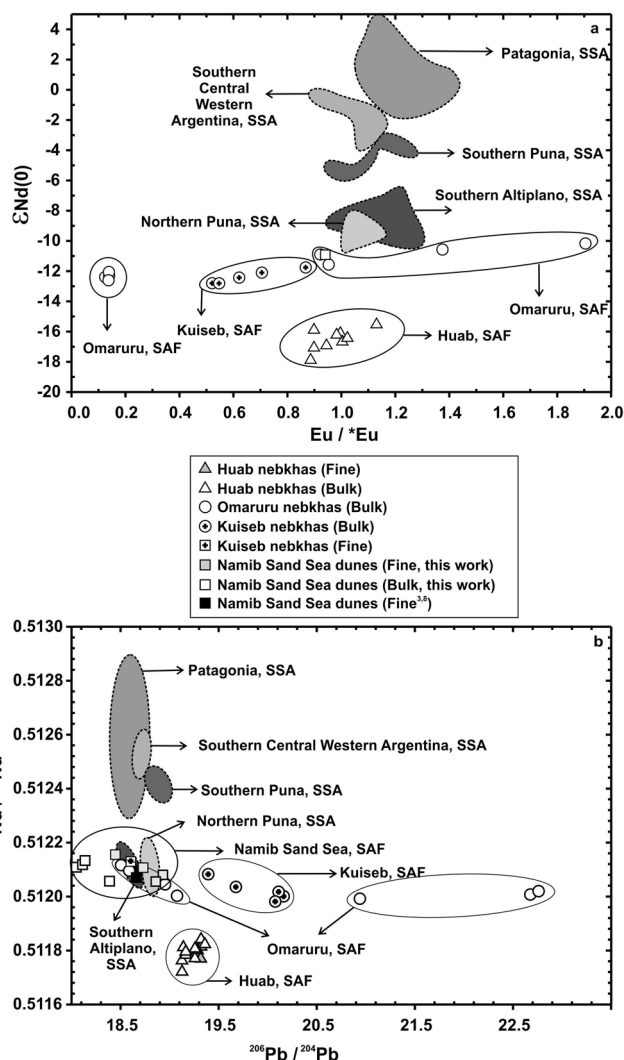


**Fig. 4 Comparison of Southern Africa (SAF) with Southern South America (SSA).** a  $\text{Eu}/^*\text{Eu}$  vs.  $\epsilon\text{Nd}(0)$ . b  $^{206}\text{Pb}/^{204}\text{Pb}$  vs.  $^{143}\text{Nd}/^{144}\text{Nd}$ . SSA data from<sup>9,10</sup>.

## Discussion

For over three decades, Sr–Nd–Pb isotopes in combination with chemical, physical, and modeled studies have focused on the provenance of dust recovered from East Antarctica ice cores. Compelling evidence has attributed Southern South America as the primary source of dust to Antarctica during both, cold and warmer periods<sup>3,5,9,10,18,49,50</sup>. Nevertheless, it is also well known that significant overlaps between the different Sr–Nd–Pb isotopic fields defining key dust areas of SSA, AUS, and NZ occur. The isotopic data presented in this study for the Southern Africa PSAs is not the exception to the imbrication issue because SAF shares some similarities in chemical/isotopic composition with some SSA PSAs (Fig. 4).

Nevertheless, the SAF and SSA signatures can be partially discriminated by combining REE with isotope data. Overall, SAF dust sources evidence very low  $\epsilon\text{Nd}(0)$  values (lower than  $-10$ ), and more radiogenic values of  $^{206}\text{Pb}/^{204}\text{Pb}$  and  $^{207}\text{Pb}/^{204}\text{Pb}$ , reflecting the signature of the Damara basement (Fig. 4a, b). In terms of REE, Huab and Kuiseb sediments exhibit an average  $\text{Eu}/\text{Eu}^* < 1$ , while Omaruru appears divided in two groups of samples; one following the same trend with  $\text{Eu}/\text{Eu}^* < 1$  and another group with scattered data, showing higher values of  $\text{Eu}/\text{Eu}^*$  (Fig. 4a). Contrarily, SSA exhibits a fingerprint that varies from

more “mafic-like” compositions from Patagonia, reflected by  $\text{Eu}/\text{Eu}^*$  values  $>1$ , higher  $^{143}\text{Nd}/^{144}\text{Nd}$  and lower  $^{206}\text{Pb}/^{204}\text{Pb}$ , in contrast with more “crustal-like” compositions of material from the Puna–Altiplano Plateau area<sup>9,10</sup> (Fig. 4a, b). In terms of  $^{143}\text{Nd}/^{144}\text{Nd}$  and  $^{206}\text{Pb}/^{204}\text{Pb}$  isotope ratios, the Namib Sand Sea data reveals a similarity with some areas of SSA, overlapping with the Southern Altiplano and Northern Puna isotopic composition fields (Fig. 4b).

The similar geochemical composition exhibited by the surface sediments of these two areas (i.e. SAF and the PAP) could be related to the comparable climatological conditions both, the Puna–Altiplano Plateau and Southwestern Africa share from their tropical to subtropical location (between about 17° and 30°S latitude). These regions are influenced by atmospheric circulation dominated by subsidence air zones (SE Atlantic–Namibia- and SE Pacific–PAP-), promoting extreme arid conditions and producing the world’s desert lands. Reinforcing the aridity in these areas is the presence of an upwelling, north-flowing, cold oceanic currents; the Humboldt current along the west coast of South America and the Benguela current along western South Africa. Precipitation is the result of tropical convection and rainfall patterns are controlled by the South American summer monsoon (SASM) and East African summer monsoon (EASM), respectively. Both areas have also shown important climatic variability during the late Quaternary, indicating altering cycles of wet/dry conditions, however interpretations about the main factors determining these changes are still controversial. Some authors have pointed to a precessional orbital control after finding a correlation between periods of Southern Hemisphere maximum insolation and enhancement of moist air on land, increasing precipitation delivered by the SASM and EASM<sup>51–53</sup>. Others have suggested that southwestern Africa responds to variations in phase with the Northern Hemisphere summer insolation<sup>54</sup>. Despite the debate of these complex mechanisms, there is persuasive evidences supporting the important role of both the PAP and SAF regions as dust suppliers during the late Quaternary. The arid and dry environmental conditions in Namibia have been similar to what it is today for the last 50 Ky, with the late Holocene being the driest period<sup>54</sup>. In addition, a pollen marine record indicated two arid peak periods (14–12 Ky and 11–9 Ky) for the early Holocene in this part of the Southern African continent<sup>55</sup>. Authors suggested a northward migration (from its present position) of the intertropical convergence zone (ITCZ) resulted in a reduction of the water vapor supply in southern subtropical Africa during the early Holocene. A marine grain-size record and a collection of terrestrial records also suggested arid conditions in southern Africa during interglacial stages due to meridional shifts in the atmospheric circulation system<sup>56,57</sup>. In line with this, a more recent pollen record from the southern Namib Desert obtained from rock hyrax middens have shown the Holocene was a time were high temperatures and evapotranspiration resulted in increased aridity and an expansion of the desert vegetation<sup>58</sup>. These environmental conditions of dryness during interglacial times are also indicated for the PAP area<sup>10</sup>, especially during the Holocene<sup>59,60</sup> and MIS 5.5<sup>61</sup>. In addition, a combined grain-size study of two marine cores taken off the coast of southwestern Africa (~20S) and western South America (~27S), observed that both sites showed arid conditions for at least the last 35,000 Ky<sup>62</sup>.

Subsequently, how the SAF fingerprint compares respect to AUS and NZ signatures is necessary to better understand the provenance of dust reaching the SO and EA. Recent studies have reviewed in detail the location, geology, atmospheric circulation patterns, and geochemical signature of all different AUS and NZ Potential Source Areas<sup>21,22,24</sup>. These studies have also thoroughly examined the geochemical fingerprint of both Australian and

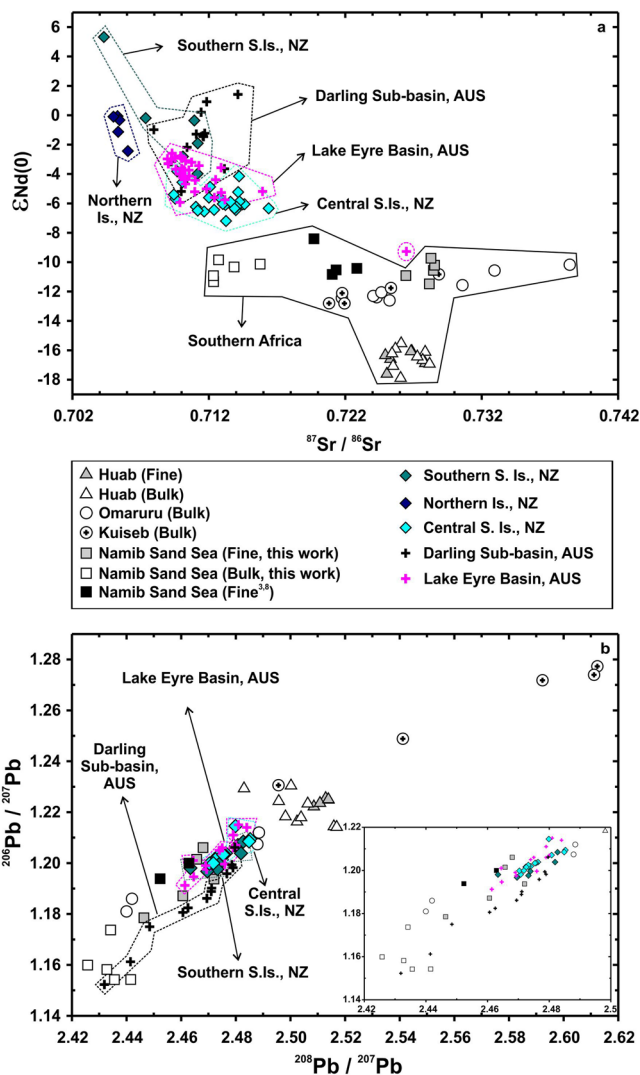


**Fig. 5 Comparison of Southern Africa (SAF) with Australia (AUS) and New Zealand (NZ) geochemical signatures. a**  $^{87}\text{Sr}/^{86}\text{Sr}$  vs.  $\epsilon\text{Nd}(0)$ . **b**  $^{208}\text{Pb}/^{207}\text{Pb}$  vs.  $^{206}\text{Pb}/^{207}\text{Pb}$ . Lake Eyre Basin, AUS data from<sup>13,21,24</sup>; Darling Sub-basin, AUS data from<sup>8,84</sup>; NZ data from<sup>3,24</sup>.

New Zealand sediments with the signature of Southern South America samples<sup>9,10</sup>, concluding that AUS and NZ sources cannot easily be distinguished from the dust sources regions of SSA. Here, for comparison against the Southern Africa signature, we use the Sr–Nd–Pb isotope ratios of the Australian and New Zealand PSAs that are relevant for comparison with ice cores records from E. Antarctica. These are: the Kati Thanda–Lake Eyre region, and the Darling Riverine Sub-Basin in Australia and New Zealand’s South Island<sup>21,22,24</sup>. As previously mentioned, Southern Africa’s diverse geology leads to a large range of Sr–Nd–Pb isotope ratios. However, these clearly differ from the AUS and NZ values and they can easily be distinguished from one another as end-members (Fig. 5a, b). Southern Africa sediments have higher  $^{87}\text{Sr}/^{86}\text{Sr}$  ( $>0.719$ ), lower  $\epsilon\text{Nd}(0)$  values ( $<-8$ ) and higher  $^{208}\text{Pb}/^{207}\text{Pb}$  ( $>2.47$ ) compared to AUS and NZ samples<sup>21,24</sup>.

Based on major/trace and Sr–Nd–Pb isotope ratios, New Zealand was indicated as a not significant dust contributor to E. Antarctica<sup>24</sup>. In contrast, these authors also found that the composition of marine sediments in the Pacific sector of the Southern Ocean (and by extension to West Antarctica) during the Holocene can be explained by a mixing of New Zealand South and North Islands with potential contributions from Lake Eyre

Basin in Australia, if dust from this latter region is able to reach the Pacific sector independently of other Australian sources.

Regarding Australia, the potential of this region to reach the Antarctic continent is still a matter a debate mainly due to that both AUS and some SSA PSAs share a similar isotopic signature with the Antarctic dust fingerprint. In this regard, a recent study has reviewed this specific subject in detail concluding that while the Southern South America signature is the predominant signature found in Antarctica, the two AUS PSAs that could have contributed dust to Antarctica are the Kati Thanda-Lake Eyre region, and the Darling Riverine Sub-Basin with the western Antarctic sites being more in favor (due to their position respect to the source)<sup>22</sup>. These two main dust regions in AUS (Supplementary Fig. 2) share a similar isotopic composition with those SSA areas identified as main dust suppliers to E. Antarctica during glacial/interglacial periods (Patagonia, Southern Central Western Argentina and the PAP) and, also show some correspondence with a few E. Antarctica glacial/interglacial samples. Moreover, only samples from the Kati Thanda-Lake Eyre region could explain the composition of a few Antarctic samples. Minor contributions from Lake Eyre have been previously suggested<sup>13,63</sup>, although the mechanism for the long-range dust transportation to Antarctica was not given. In fact, based on HYSPLIT models, there is only one study (to the best of our knowledge) that showed that during spring months when dust from Lake Eyre is entrained by warm and dry northwesterly winds, could potentially be transported to certain Antarctic sectors such as, George V Land, and to a lesser extent, the peninsula within eight days<sup>64</sup>. However, the isotopic composition of Lake Eyre doesn't match with the Sr-Nd isotopic ratios of modern dust measured at Berkner Island, Antarctic Peninsula<sup>41</sup> (Supplementary Fig. 2). Furthermore, AGCMs have shown that during both climatic periods present-day and the LGM, AUS 'tracers' are/were highly concentrated in West Antarctica sectors, particularly in Mary Byrd Land<sup>19</sup>. Although, a description of which AUS sources were used in the study was not provided. It should also be noted that due to the geographic distribution, Australian dust gets well-mixed before reaching the southeast Australian coastline. This is; the AUS PSAs come across a narrow latitudinal strip but a broad longitudinal area which has important implications for the dust mobilization in the region mainly associated with easterly fronts within the westerly wind belt<sup>13</sup>. Hence, when dust events occur, different AUS PSAs can be picked up as a whole and the result is a dust plume with a very similar and comparable Australian fingerprint<sup>13,65,66</sup>. Thus, while it is clear that based on the Sr-Nd-Pb combination approach we cannot dismiss the possibility of a minor contribution of Australian dust to Antarctica, especially to West Antarctica, it is also true that the processes on how dust from the Lake Eyre is/was transported to East Antarctica is not fully understood yet and more research in this topic is needed. With these observations made above, is that this study does not consider AUS as an important end-member contributing dust to E. Antarctica.

Based on Sr-Nd-Pb isotopes, only two earlier studies<sup>3,8</sup> suggested the possibility of SAF as a PSA to the polar Antarctic regions. However, due to the limited number of sediment samples and their distinct geochemical signature with respect to EA, they concluded isotopic data was not conclusive enough to support a dust contribution from SAF, excluding this region from the provenance puzzle. Contrarily, the new and expanded dataset of Southern Africa Sr-Nd-Pb isotopic ratios and REE concentrations presented in this study indicate that, SAF emerges as PSA that together with high-latitudes sources in Southern South America (i.e., Patagonia, Southern Central Western Argentina, and the Puna–Altiplano Plateau) can explain the glacial/interglacial dust signature observed in East Antarctica ice cores, as well as the

signature of marine sediments from the South Atlantic sector of the Southern Ocean (Fig. 6).

In general, the  $^{87}\text{Sr}/^{86}\text{Sr}$  and  $\epsilon\text{Nd}(0)$  values are more diagnostic than the  $^{206,208}\text{Pb}/^{207}\text{Pb}$  for identifying the glacial/interglacial dust provenance in paleo-archives. This means that even though the Pb isotopic data is usually less indicative because of the Pb input related to local (Antarctic) volcanoes in comparison to the dust related Pb<sup>8</sup>, the Pb data in the present study add critical support to our interpretations. This is, the new Pb isotope data of SAF samples define a field that, together with Southern South America PSAs can better explain the entire range of Pb isotopic compositions observed in the East Antarctic dust from Vostok and EDC ( $^{208}\text{Pb}/^{207}\text{Pb}$  values from 2.44–2.50) (Fig. 6a). It should also be noticed that the very radiogenic Pb data similar to Kuseib envelope are also those of the Antarctic local volcanoes (Mt. Erebus); contribution that has been recognized in previous studies<sup>8,9,67</sup> and cannot be denied. Thus, our results show that EA dust samples show two main compositional trends that comprise different end-members (orange dashed lines in Fig. 6b). This is, a common end-member with low values in both  $^{208}\text{Pb}/^{207}\text{Pb}$ , and  $^{206}\text{Pb}/^{207}\text{Pb}$  elucidated by either the Namib Sand Sea (fine fraction) or the Patagonia/Southern Central Western Argentina sources in combination with a more radiogenic end-member, that is, either Kuseib PSA or the local Antarctic volcanism with a contribution from the Puna Altiplano Plateau (PAP) and the Huab region, especially during interglacial times (Fig. 6b).

This is also in part supported by Sr and Nd isotopic data (Fig. 6c, d), where the new SAF dataset defines a compositional field that turns out to be a key end-member for describing the composition of dust deposited in the South Atlantic and East Antarctica. In general, during the last glacial climatic periods of the late Quaternary, EA data is very uniform converging to an unequivocal signature from Patagonia with additional inputs from other lower latitude areas in SSA, such as, the Southern Central Western Argentina (SCWA) and Southern Puna<sup>10</sup> (Fig. 6c). On the other hand, the EA interglacial dust fingerprint, as well as the glacial/interglacial signature of marine sediments from the South Atlantic are marked by a variable mix of sources (Fig. 6c). An important finding of this study is that a tri-mixing hyperbola with two common end-members can be drawn and help to decipher this variability. This is, the best candidates to elucidate the origin of dust during the Holocene and likely during the last 15 ka are a more mafic-like end-member represented by Patagonia and/or SCWA, in addition to a second crustal-like end-member, defined by the Southern Altiplano, plus a third end-member, which can either be the Northern Puna (black solid line) and/or Southern Africa region as a whole (dotted black line) (Fig. 6d, Supplementary Table 1). This is also in agreement with the isotopic composition of present-day dust deposited on the Berkner Island in the Atlantic sector of coastal Antarctica, which can clearly be ascribed to a mixing isotopic composition from PAP<sup>10,41</sup>, and SAF PSAs (Fig. 6d). It was also suggested that neither of the PSAs in SSA could account for the entire Sr-Nd isotopic range of the dust deposited on Berkner and that the contribution of another secondary source with more negative  $\epsilon\text{Nd}(0)$  was missing<sup>41</sup>. The Sr and Nd signature of the SAF samples presented here can account for that 'missing' end-member, although local sources cannot be dismissed. Alike, it was inferred that the Holocene signature identified in ocean sediments from the Atlantic sector of the Southern Ocean is associated with material derived from SAF, but also with compositions similar to the Northern Puna<sup>68</sup> (Fig. 6c, d). Moreover, detrital Nd isotopic composition of marine sediments recovered in the South Atlantic region, right off the Namibia coast, have shown  $\epsilon\text{Nd}(0)$  values between  $-10$  and  $-22$  that have been attributed to a Southern Africa origin<sup>69</sup>, which is in accordance with the new Neodymium



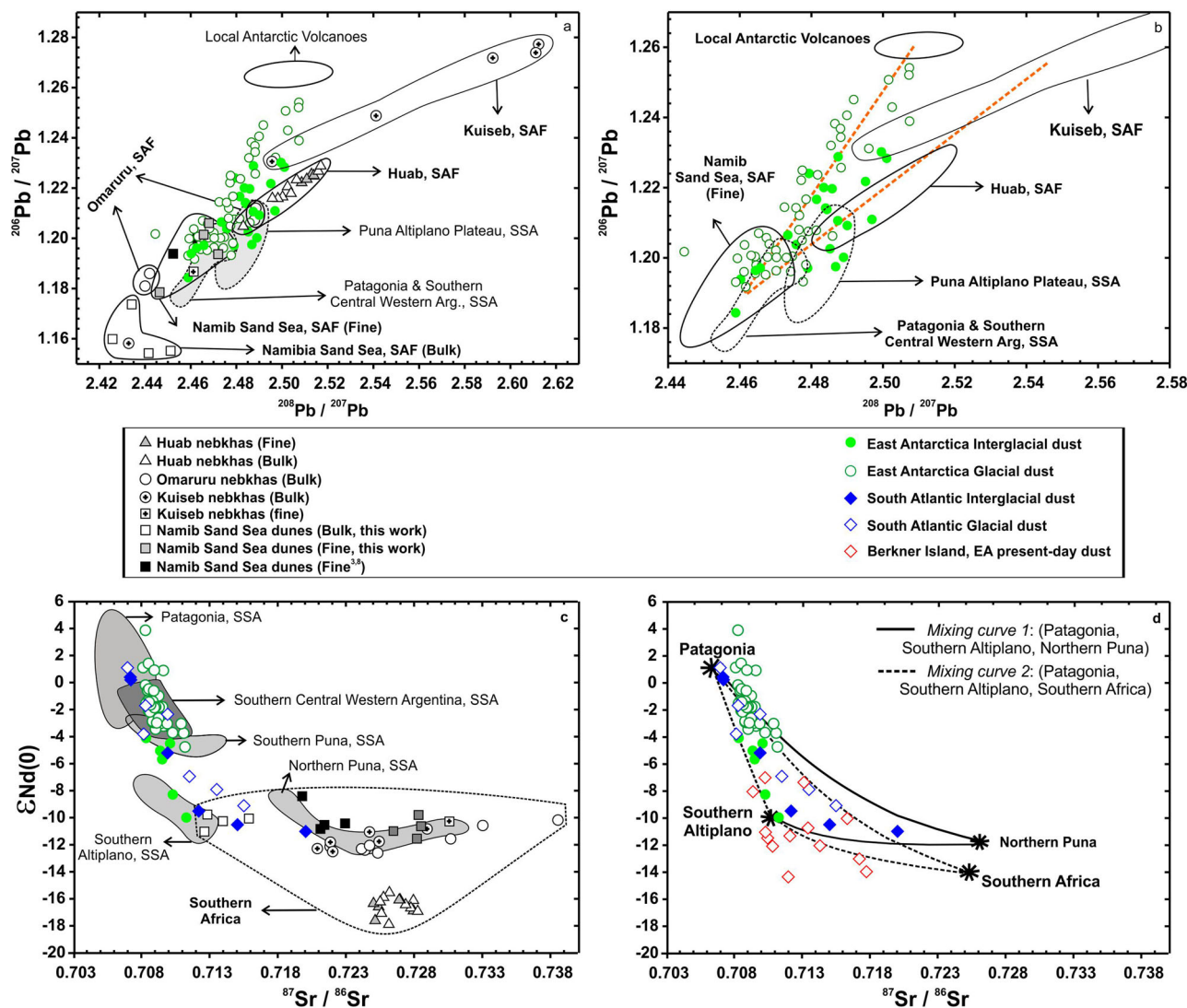


**Fig. 6** Comparison of Southern Africa (SAF) and Southern South America (SSA) isotopic signatures with the glacial/interglacial fingerprint of dust deposited in East Antarctica and the South Atlantic sector of the Southern Ocean. **a**, **b**  $^{208}\text{Pb}/^{207}\text{Pb}$  vs.  $^{206}\text{Pb}/^{207}\text{Pb}$ . The orange dotted lines in Fig. 6b represent compositional trend lines necessary to explain EA dust compositions. **c**, **d**  $^{87}\text{Sr}/^{86}\text{Sr}$  and  $\epsilon\text{Nd}(0)$ . The black lines in Fig. 6d represent the calculated tri-mixing hyperbola between different PSAs of SAF (dotted line) and SSA (fill line). End-member values used to calculate Sr–Pb mixing curves can be found in Supplementary Table 1. Local Antarctic Volcanoes data in Fig. 6a is from<sup>8</sup>. SSA data from<sup>9,10</sup>. East Antarctica glacial/interglacial data from<sup>3,5,8,63,70,85</sup>. Berkner Island data from<sup>41</sup>.

isotopic data presented in this study. Authors associated trade-winds as the main mechanism responsible of transporting detrital material to the South Atlantic Ocean. Likewise, another marine core recovered from the Walvis Ridge pointed the Berg winds as another possible transport mechanism for the aeolian dust sweeping away from the Namibia coast<sup>56</sup>. The same study revealed that SAF climate was relatively arid during the interglacial stages and relatively humid during the glacial stages. During glacial stages, the polar front shifted equatorward resulting in a northward displacement of the westerlies belt, causing increased rainfall in southwestern Africa<sup>55</sup>. This could help explain why the signature of SAF PSAs may have had a lesser role during cold periods in comparison with warmer periods when the activation of other sources, such as the Puna–Altiplano Altiplano Plateau and SAF prevail. Additionally, the strong Southern Central Western Argentina fingerprint seen in glacial dust deposited in EA agreed with an overall equatorward displacement of the mid-latitude westerlies during glacial times<sup>10</sup>.

While the geochemical evidences presented here demonstrate that SAF sediments and interglacial/modern dust deposited in different environments of the Southern Hemisphere (SH) share a similar isotopic signature, the concept about how the transport occurs from the Namibian coastal regions to Antarctica is still not well known. The deposition of dust around Antarctica can happen by either a scenario whereby it is deposited in the interior high elevation sites or in the periphery low elevation sites of the Antarctic plateau<sup>70</sup>. Mineral dust reaching the EA plateau is windborne long-range transported from the continental landmasses carried through the mid-to high troposphere. For dust sources that are not located at high latitudes, such as the case of SAF, there is need of strong convective uplift of particles up to 200–400 mbar to reach the interior plateau and the presence of SAF particles has mostly been reported in the lower troposphere<sup>71</sup>. Another possibility is that the source itself is already elevated in altitude allowing the injection of dust particles directly in the high troposphere. This is the case of the



Puna–Altiplano Plateau in SSA, where the subtropical jet stream acts as main mechanism mobilizing large amounts of dust that ultimately, get deposited onto the polar plateau<sup>7,10,12</sup> and whose signal has also been found in peripheric areas of Antarctica in the Berkner Island<sup>41</sup>. Modeling data have suggested that material from SAF only contributes with ~5% of the total dust burden over Antarctica and a southward transport to the inner part of the Antarctic continent would be unlike<sup>18,20</sup>. However, modeled dust emission fluxes from the different PSAs of the SH and their subsequent deposition driven by the local trade winds, can vary by as much as a factor of four or more, which could mislead to controversial interpretations<sup>23</sup>. This has important implications especially at ice core sites located on the high-elevated plateau areas (~3000–4000 m) that can be particularly isolated from extra-Antarctic dust sources, and where AGCM experiments struggle to reproduce dust concentrations in ice core samples<sup>18,20,72</sup>. While recognizing the limitations of modeling in representing the global dust cycle, a more recent study introduced a novel tool known as DustCOMM (Dust Constraints from joint Observational-Modelling-experimental analysis)<sup>73</sup>; a continuously expanding dataset of constraints on the global dust cycle that combines observational and experimental analyses on dust properties and dust abundance with an ensemble of global aerosol model simulations. DustCOMM showed that while SSA accounts for the large majority (70%) of the dust deposited in almost the entire Antarctic continent, smaller contributions from Australia (20%) and southern Africa (10%) are also observed<sup>73</sup>. The work done by Neff and Butler (2015) also indicated that the dust contribution from SAF sources located in the arid regions of Namibia, is significant in Southern Ocean areas off the Antarctic coast near Wilkes Land, E.A, and at Law Dome. Using HYSPLIT, a trajectory model, another study showed that dust emissions from the Southern Kalahari commonly reach the Southern Ocean<sup>74</sup>, with most of the trajectories traveling beyond 40°S during the dry period (April–September) when conditions favor the dust production and transportation<sup>75</sup>.

We note however, that most of the regional to global dust modelings regarding Namibian sources are solely based on the atmospheric circulation of the trade winds to emit dust. While in reality, it is the Berg winds, a local southwestern Africa topographically enhanced thermal wind that represents a more important driving force responsible of dust mobilization and deposition over the ocean<sup>28,76</sup>. These hot and dry winds are also more common in winter and they are the result of adiabatic heating; a process that occurs when air coming from the escarpment and plateaus descends towards the Namibian coastline, getting compressed and heated. Multiple dust streams and dust storms originated in this part of the African continent evidencing the substantial transport of material to the Southern Ocean as a result of Berg winds have been spotted by different satellite platforms<sup>28,29</sup>. This has important implications for the transportation of material to the marginal and coastal sites of Antarctica, which can receive an unquantified amount of SAF dust. On this matter, more recent studies have showed strong support that highlights Southern Africa as a secondary and significant dust supplier to East Antarctica. Sr, Nd and Pb isotope ratios of Antarctic modern dust recovered from snow samples collected along coastal sites of the Dronning-Maud Land area (DML-East Antarctica), have shown similar composition to the Southern Africa sediments<sup>77</sup>. This data is consistent with the results observed using back trajectory FLEXPART particle dispersion transport model where a mix of modern Southern Africa and Southern South America dust sources was clearly spotted in the coastal area of East Antarctica<sup>78</sup>. Likewise, using a statistical analysis a study revisited the only EDML ice core rare earth elements dataset available from<sup>17</sup>, and observed that the Southern

Africa fingerprint appears at ~15 ky as an important mixing end-member that together with SSA, can explain the East Antarctica interglacial dust signature<sup>79</sup>. Ultimately, another geochemical study carried out in a core from the Southern Indian Ocean, has also proposed a mixing model where SSA and SAF have been found to be the main distal dust sources through most of the Holocene<sup>80</sup>.

In resumé, this study agrees with previous findings suggesting that SSA is the best candidate to explain the dust signature recorded in the SO and EA during cold and warm stages. For warm periods, this study proposes a scheme where the typical isotopic variability observed in interglacial and present-day dust depositions in the South Atlantic Ocean and coastal regions of East Antarctica can be related to the contributions of two main PSAs: Southern South America, through westerlies dominating the atmospheric circulation over Patagonia and Southern Central Western Argentina and, the jet stream over the Puna–Altiplano Plateau, in combination with Southern Africa in response to the plausible transport by strong Berg winds. We rely in part on an understanding of modern wind-dust activities showed by satellite images to conclude the possible contribution of Southern Africa dust emissions during interglacial times. However, modeling studies focusing on the interplay between the southeast trade-winds, and Berg winds that dominate dust transportation off the Namibian coast and the extent of this transport to higher latitude areas, are immensely needed.

## Methods

Acknowledging the location of the main dust sources of the areas investigated in this study, nebkhas and sand dunes were sampled along the lower valleys of the Huab, Omaruru, and Kuiseb river systems and the Namib Sand Sea (Fig. 1a, blue diamonds. See Supplementary Table 1 for more details). Aiming to evaluate the provenance and long-range transportation of dust from these Southern Africa PSAs and depositions in remote areas, a total of 22 bulk samples (nine samples from Huab, seven from Omaruru and six from Kuiseb) were analyzed in terms of their REE concentrations and Sr-Nd-Pb isotope compositions. Additionally, measurements of Sr-Nd-Pb isotope ratios were carried out in five bulk and five fine (<5 µm) fraction samples from the Namib Sand Sea, to produce a comparable result to the bulk samples previously analyzed in<sup>3,8</sup>. Furthermore, to assess a possible change in the geochemical fingerprint due to grain-size effects, six bulk samples from the Huab valley were selected to generate airborne aerosols dust in the fine fraction (~<11 µm) using an atmospheric simulation chamber (see section 4.1 and supplementary materials for further details). The aerosol fraction investigated in this study has also important implications for provenance studies as only certain particle sizes can be transported long distances. Hence, analyzing the right size fraction in the source region is crucial to identify the origin of dust reaching the Southern Ocean and Antarctica.

**Sample collection.** According to remote sensing analyses, the most persistent dust sources in the Huab region are concentrated upstream of the river catchment; this is, in the river flood channel itself, in a playa and a delta. Dust sources are associated with fluvial silt crust terraces covered with nebkhas. In the case of the silt crust, these surfaces will only emit dust if an erodible material such as sand is present to initiate the saltation. The nebkhas in the delta section of the Huab River, present almost no vegetation cover making them a source of aeolian sediments that is picked up not only by the high magnitude north-easterly Berg winds, but also during the predominant southerly winds<sup>28,29</sup>. In Omaruru, most of the dust emissions (>80%) happen downstream within the floodplain channel of the river as a result of the high-magnitude northeast winds. Nebkhas and degraded silt crusts are the two main landforms in the terrain, with the nebkhas being the major source for dust deflation due to the sparse vegetation they present which results in poor protection against the wind<sup>29</sup>. For the Kuiseb, the silt-clay fines are deposited in the lower sections of the river becoming silt crusts that are the dominant source of dust through saltation, erosion and suspension. As for the Huab river, saltation is the mechanism responsible of dust entrainment and emission<sup>28,29</sup>.

With this in mind, small vegetated dunes (nebkhas) were targeted to be a representative sample of that particular basin for currently active transport at a distance from the ocean. For the Huab and Omaruru, the sites were uniform in terms of landform. These were nebkhas with loose sediment around their bases that the surface sediment was sampled ('last remaining dust stores'). In the case of the Kuiseb, silt-fine material was sampled. These vegetation-free Nebkhas are located where the Namib Sand Sea and the silt terraces from the river meet, and where the processes involving these two sediment sources (but most importantly the presence of the silt terraces from the river) are what makes this area so dusty. Thus, bulk

surface samples from Huab, Omaruru and Kuiseb riverbeds were collected in a field camping in August 2017, using a trowel to obtain approximately 200 g of sediment from the surface. Sub-samples of ~350 mg were stored in pre-cleaned centrifuges tubes and shipped to Université Libre de Bruxelles (ULB), Belgium for analysis. From the bulk of six samples from Huab, dust aerosols (fine fraction) were generated into the CESAM atmospheric simulation chamber, to mechanically reproduce the saltation and sandblasting processes responsible for the release of mineral dust in natural conditions<sup>81</sup>. Briefly, dust aerosols are generated from the bulk sediments by a mechanical shaker and the aerosols are injected into the CESAM chamber<sup>82</sup>, a stainless-steel reactor with a volume of 4.2 m<sup>3</sup> where dust is dispersed, left in suspension for ~3 h, and ultimately recovered on acid-cleaned 0.2 µm Teflon filters. Additional details about the dust generation in the CESAM are provided in the Supplementary Methods. Samples from the Namib Sand Sea correspond to sand dunes previously analyzed for the Sr-Nd<sup>3</sup> and Pb<sup>8</sup> isotopic composition. Here, we have re-analyzed the bulk and the fine fraction of those samples, where the fine fraction was separated using the Stoke's Law<sup>3</sup>.

**Geochemical analyses.** Sample preparation and analyses for REE elemental and, Sr-Nd-Pb isotope compositions were carried out on bulk and fine fraction samples. Sediment samples were dissolved in a concentrated HF + HNO<sub>3</sub> mixture followed by an HCl bath in Savillex vials and Sr-Nd-Pb were separated through chromatography using ion-exchange resins following the procedure reported in<sup>83</sup>. Isotopes were measured at the G-Time Lab, Université Libre de Bruxelles (Belgium) using a High-Resolution MC-ICP-MS Plasma II (Nu Instruments) in dry mode. The REE concentrations were determined using a Quadrupole ICP-MS Agilent 7700. Additional details of the analytical methodology are provided in Supplementary Methods.

### Data availability

The satellite image used in Fig. 1 can be found on the NASA visible earth website <https://visibleearth.nasa.gov/images/81073/dust-plumes-off-namibia/81075w>. NASA image credit: Jeff Schmaltz, MODIS Rapid Response Team at NASA GSFC. All data needed to replicate the findings of the study are publicly accessible in a repository source data 10.6084/m9.figshare.19660557 and 10.6084/m9.figshare.19786345.

Received: 20 September 2021; Accepted: 20 May 2022;

Published online: 09 June 2022

### References

- Shao, Y. et al. Dust cycle: an emerging core theme in Earth system science. *Aeolian Res.* **2**, 181–204 (2011).
- Lambert, F. et al. Dust–Climate couplings over the past 800,000 years from the EPICA Dome C ice core. *Nature* **452**, 616–619 (2008).
- Delmonte, B. et al. Comparing the Epica and Vostok dust records during the last 220,000 years: stratigraphical correlation and provenance in glacial periods. *Earth-Science Rev.* **66**, 63–87 (2004).
- Grousset, F. E. et al. Antarctic (Dome C) ice-core dust at 18 k.y.B.P.: isotopic constraints on origins. *Earth and Planet. Sci. Lett.* **111**, 175–182 (1992).
- Basile, I. et al. Patagonian origin of glacial dust deposited in East Antarctica (Vostok and Dome C) during glacial stages 2, 4 and 6. *Earth and Planet Sci. Lett.* **146**, 573–589 (1997).
- Delmonte, B. et al. Holocene dust in East Antarctica: provenance and variability in time and space. *Holocene* **30**, 546–558 (2020).
- Gaiero, D. M. Dust provenance in Antarctic ice during glacial periods: from where in southern South America? *Geophys. Res. Lett.* **34**, 1–6 (2007).
- Vallelonga, P. et al. Lead isotopic compositions in the EPICA Dome C ice core and southern hemisphere potential source areas. *Quaternary Sci. Rev.* **29**, 247–255 (2010).
- Gili, S. et al. Provenance of dust to Antarctica: a lead isotopic perspective. *Geophys. Res. Lett.* **43**, 2291–2298 (2016).
- Gili, S. et al. Glacial/interglacial changes of Southern Hemisphere wind circulation from the geochemistry of South American dust. *Earth and Planet. Sci. Lett.* **469**, 98–109 (2017).
- Gaiero, D. M., Depetris, P. J., Probst, J. L., Bidart, S. M. & Leleyter, L. The signature of river- and wind-borne materials exported from Patagonia to the southern latitudes: a view from REEs and implications for paleoclimatic interpretations. *Earth and Planet. Sci. Lett.* **219**, 357–376 (2004).
- Gaiero, D. M. et al. Ground/satellite observations and atmospheric modeling of dust storms originating in the high Puna-Altiplano deserts (South America): implications for the interpretation of paleo-climatic archives. *J. of Geophys. Res.: Atmospheres* **118**, 3817–3831 (2013).
- Revel-Rolland, M. et al. Eastern Australia: a possible source of dust in East Antarctica interglacial ice. *Earth and Planet. Science Lett.* **249**, 1–13 (2006).
- Marino, F. et al. Defining the geochemical composition of the EPICA Dome C ice core dust during the last glacial-interglacial cycle. *Geochemistry Geophysics Geosystems*. <https://doi.org/10.1029/2008GC002023> (2008).
- de Deckker, P., Norman, M., Goodwin, I. D., Wain, A. & Gingeles, F. X. Lead isotopic evidence for an Australian source of aeolian dust to Antarctica at times over the last 170,000 years. *Palaeogeogr., Palaeoclimatol., Palaeoecol.* **285**, 205–223 (2010).
- Gabrielli, P. et al. A major glacial-interglacial change in aeolian dust composition inferred from Rare Earth Elements in Antarctic ice. *Quat. Sci. Rev.* **29**, 265–273 (2010).
- Wegner, A. et al. Change in dust variability in the Atlantic sector of Antarctica at the end of the last deglaciation. *Climate of the Past* **8**, 135–147 (2012).
- Li, F., Ginoux, P. & Ramaswamy, V. Distribution, transport, and deposition of mineral dust in the Southern Ocean and Antarctica: Contribution of major sources. *J. of Geophys. Res. Atmospheres* **113**, 1–15 (2008).
- Krinner, G., Petit, J. R. & Delmonte, B. Altitude of atmospheric tracer transport towards Antarctica in present and glacial climate. *Quat. Sci. Rev.* **29**, 274–284 (2010).
- Albani, S., Mahowald, N. M., Delmonte, B., Maggi, V. & Winckler, G. Comparing modeled and observed changes in mineral dust transport and deposition to Antarctica between the Last Glacial Maximum and current climates. *Climate Dynamics* **38**, 1731–1755 (2012).
- de Deckker, P. An evaluation of Australia as a major source of dust. *Earth-Sci. Rev.* **194**, 536–567 (2019).
- de Deckker, P. Airborne dust traffic from Australia in modern and Late Quaternary times. *Global and Planet. Change* **184**, 103056 (2020).
- Neff, P. D. & Bertler, N. A. N. Trajectory modeling of modern dust transport to the Southern Ocean and Antarctica. *J. of Geophys. Res.* **120**, 9303–9322 (2015).
- Koffman, B. G. et al. New Zealand as a source of mineral dust to the atmosphere and ocean. *Quater. Sci. Rev.* **251**, 106659 (2021).
- Prospero, J. M., Ginoux, P., Torres, O., Nicholson, S. E. & Gill, T. E. Environmental characterization of global sources of atmospheric soil dust identified with the Nimbus 7 Total Ozone Mapping Spectrometer (TOMS) absorbing aerosol product. *Rev. of Geophys.* **40**, 2-1-2–31 (2002).
- Bryant, R. G. Monitoring hydrological controls on dust emissions: preliminary observations from Etosha Pan, Namibia. *The Geogr. J.* **169**. [www.saa.noaa.gov/](http://www.saa.noaa.gov/) (2003).
- Mahowald, N. M. & Kiehl, L. M. Mineral aerosol and cloud interactions. *Geophys. Res. Lett.* **30**, 1475 (2003).
- Vickery, K. J. & Eckardt, F. D. Dust emission controls on the lower Kuiseb River valley, Central Namib. *Aeolian Res.* **10**, (2013).
- von Holdt, J. R., Eckardt, F. D. & Wiggs, G. F. S. Landsat identifies aeolian dust emission dynamics at the landform scale. *Remote Sens. of Environ.* **198**, 229–243 (2017).
- Jacobson, P. J., Jacobson, K. N. & Seely, M. K. Ephemeral rivers and their catchments: sustaining people and development in western Namibia. Desert Research Foundation of Namibia, Windhoek, 160 pp (1995).
- Heine, K. & Heine, J. T. A paleohydrologic reinterpretation of the Homeb Silts, Kuiseb River, central Namib Desert (Namibia) and paleoclimatic implications. *CATENA* **48**, 107–130 (2002).
- Dansie, A. P., Wiggs, G. F. S., Thomas, D. S. G. & Washington, R. Measurements of windblown dust characteristics and ocean fertilization potential: The ephemeral river valleys of Namibia. *Aeolian Res.* **29**, 30–41 (2017).
- Eckardt, F. D. et al. The nature of moisture at Gobabeb, in the central Namib Desert. *J. of Arid Environ.* **93**, 7–19 (2013).
- von Holdt, J. R. C., Eckardt, F. D., Baddock, M. C. & Wiggs, G. F. S. Assessing landscape dust emission potential using combined ground-based measurements and remote sensing data. *J. of Geophys. Res.: Earth Surf.* **124**, 1080–1098 (2019).
- Eckardt, F. D. et al. South Africa's agricultural dust sources and events from MSG SEVIRI. *Aeolian Res* **47**, 100637 (2020).
- Compton, J. S., Herbert, C. T., Hoffman, M. T., Schneider, R. R. & Stuu, J.-B. A tenfold increase in the Orange River mean Holocene mud flux: implications for soil erosion in South Africa. *Holocene* **20**, 115–122 (2010).
- Jickells, T. D. et al. Global iron connections between desert dust, ocean biogeochemistry, and climate. *Science* **308**(67–71), 2005 (1979).
- Jury, M. R. Physical and oceanographic influences on Central Benguela fish catch. *Earth Interact.* **16**, 1–15 (2012).
- Lancaster, N. & Ollier, C. D. Sources of sand for the Namib Sand Sea. *Zeitschrift für Geomorphologie Supplementband* **45**, 71–83 (1983).
- Tlhalerwa, K., Freiman, M. T. & Piketh, S. J. Aerosol deposition off the southern african west coast by berg winds. *South African Geogr. J.* **87**, 152–161 (2005).
- Bory, A. et al. Multiple sources supply eolian mineral dust to the Atlantic sector of coastal Antarctica: Evidence from recent snow layers at the top of Berkner Island ice sheet. *Earth and Planet. Sci. Lett.* **291**, 138–148 (2010).

42. Garzanti, E. et al. Ultra-long distance littoral transport of Orange sand and provenance of the Skeleton Coast Erg (Namibia). *Marine Geol.* **357**, 25–36 (2014).
43. Goscombe, B. D., Hand, M. & Gray, D. R. Structure of the Kaoko Belt, Namibia: progressive evolution of a classic transpressional orogen. *J. of Struct. Geol.* **25**, 1049–1081 (2003).
44. Taylor, S. R. (via)108589885 & McLennan, S. M. (via)67975976. The continental crust: its composition and evolution: an examination of the geochemical record preserved in sedimentary rocks. (Oxford: Blackwell scientific, 1985).
45. Bayon, G., German, C. R., Burton, K. W., Nesbitt, R. W. & Rogers, N. Sedimentary Fe–Mn oxyhydroxides as paleoceanographic archives and the role of aeolian flux in regulating oceanic dissolved REE. *Earth and Planet. Sci. Lett.* **224**, 477–492 (2004).
46. Miller, R. M. *The Geology of Namibia*. (Minister of Mines and Energy, Windhoek, 2008). vol. 3.
47. Garçon, M., Chauvel, C., France-Lanord, C., Limonta, M. & Garzanti, E. Which minerals control the Nd–Hf–Sr–Pb isotopic compositions of river sediments? <https://doi.org/10.1016/j.chemgeo.2013.11.018> (2014).
48. Bayon, G. et al. Rare earth elements and neodymium isotopes in world river sediments revisited. *Geochimica et Cosmochimica Acta* **170**, 17–38 (2015).
49. Gaiero, D. M., Brunet, F., Probst, J. L. & Depetris, P. J. A uniform isotopic and chemical signature of dust exported from Patagonia: Rock sources and occurrence in southern environments. *Chem. Geol.* **238**, 107–120 (2007).
50. Albani, S. et al. Climate of the past discussions interpreting last glacial to holocene dust changes at Talos Dome (East Antarctica): implications for atmospheric variations from regional to hemispheric scales. *Clim. Past Discuss* **8**, 145–168 (2012).
51. Partridge, T. C., Demenocal, P. B., Lorentz, S. A., Paiker, M. J. & Vogel, J. C. Orbital forcing of climate over South Africa: a 200,000-year rainfall record from the pretoria saltpan. *Quater. Sci. Rev.* **16**, 1125–1133 (1997).
52. Baker, P. A. et al. Tropical climate changes at millennial and orbital timescales on the bolivian Altiplano. *Nature* **409**, 698–701 (2001).
53. Fritz, S. C. et al. Hydrologic variation during the last 170,000 years in the southern hemisphere tropics of South America. *Quater. Res.* **61**, 95–104 (2004).
54. Chase, B. M. et al. Orbital controls on Namib Desert hydroclimate over the past 50,000 years. *Geology* **47**, 867–871 (2019).
55. Shi, N., Dupont, L. M., Beug, H. J. & Schneider, R. Correlation between vegetation in Southwestern Africa and oceanic upwelling in the past 21,000 years. *Quater. Res.* **54**, 72–80 (2000).
56. Stuut, J. B. W. et al. A 300-kyr record of aridity and wind strength in southwestern Africa: inferences from grain-size distributions of sediments on Walvis Ridge, SE Atlantic. *Mar. Geol.* **180**, 221–233 (2002).
57. Chase, B. M. & Meadows, M. E. Late Quaternary dynamics of southern Africa's winter rainfall zone. *Earth-Sci. Rev.* **84**, 103–138 (2007).
58. Lim, S., Chase, B. M., Chevalier, M. & Reimer, P. J. 50,000 years of vegetation and climate change in the southern Namib Desert, Pella, South Africa. *Palaeogeogr., Palaeoclimatol., Palaeoecol.* **451**, 197–209 (2016).
59. Fornace, K. L. et al. A 60,000-year record of hydrologic variability in the Central Andes from the hydrogen isotopic composition of leaf waxes in Lake Titicaca sediments. *Earth and Planet. Sci. Lett.* **408**, 263–271 (2014).
60. Torre, G., Gaiero, D. M., Cosentino, N. J., Coppo, R. & Oliveira-Sawakuchi, A. New insights on sources contributing dust to the loess record of the western edge of the Pampean Plain during the transition from the late MIS 2 to the early Holocene. *Holocene* **30**, 537–545 (2020).
61. Baker, P. A. & Fritz, S. C. Nature and causes of Quaternary climate variation of tropical South America. *Quater. Sci. Rev.* **124**, 31–47 (2015).
62. Stuut, J. B. W. & Lamy, F. Climate variability at the southern boundaries of the Namib (southwestern Africa) and Atacama (northern Chile) coastal deserts during the last 120,000 yr. *Quater. Res.* **62**, 301–309 (2004).
63. Delmonte, B. et al. Geographic provenance of aeolian dust in East Antarctica during Pleistocene glaciations: preliminary results from Talos Dome and comparison with East Antarctic and new Andean ice core data. *Quater. Sci. Rev.* **29**, 256–264 (2010).
64. McGowan, H. & Clark, A. Identification of dust transport pathways from Lake Eyre, Australia using Hysplit. *Atmos. Environ.* **42**, 6915–6925 (2008).
65. Raupach Canberra (Australia). Centre for Environmental Mechanics), M. (Commonwealth S. and I. R. O., McTainsh Nathan (Australia), Faculty of Environmental Sciences), G. (Griffith Univ. & Leys Gunnedah (Australia)), J. (New S. W. C. and L. M. Estimates of dust mass in recent major Australian dust storms. Australian Journal of Soil and Water Conservation (Australia) vol. v. 7.
66. de Deckker, P. & Norman, M. D. Re-evaluation of the composition of sediments from the Murray Darling Basin of Australia as a Potential Source Area for airborne dust to EPICA Dome C in Antarctica. Reply to Comment on “Lead isotopic evidence for an Australian source of aeolian dust to Antarctica at times over the last 170,000 years” by P. De Deckker, M. Norman, I.D. Goodwin, A. Wain and F.X. Gingele [Palaeogeography, Palaeoclimatology, Palaeoecology 285 (2010) 205–223]. *Palaeogeogr., Palaeoclimatol., Palaeoecol.* **298**, 437–442 (2010).
67. Hinkley, T. Lead (Pb) in old Antarctic ice: some from dust, some from other sources. *Geophysical Research Letters* **34**, L08502 (2007).
68. Noble, T. L. et al. Greater supply of Patagonian-sourced detritus and transport by the ACC to the Atlantic sector of the Southern Ocean during the last glacial period. *Earth and Planet. Sci. Lett.* **317–318**, 374–385 (2012).
69. Bayon, G., German, C. R., Nesbitt, R. W., Bertrand, P. & Schneider, R. R. Increased input of circumpolar deep water-borne detritus to the glacial SE Atlantic Ocean. *Geochem., Geophys., Geosyst.* **4**, 1025 (2003).
70. Delmonte, B. et al. Aeolian dust in East Antarctica (EPICA-Dome C and Vostok): Provenance during glacial ages over the last 800 kyr. *Geophys. Res. Lett.* **35**, L07703 (2008).
71. Chazette, P. et al. Evidence of the complexity of aerosol transport in the lower troposphere on the Namibian coast during AEROCLO-sA. *Atmos. Chem. and Phys.* **19**, 14979–15005 (2019).
72. Mahowald, N. et al. Dust sources and deposition during the last glacial maximum and current climate: a comparison of model results with paleodata from ice cores and marine sediments. *J. of Geophys. Res. Atmos.* **104**, 15895–15916 (1999).
73. Kok, J. et al. Contribution of the world's main dust source regions to the global cycle of desert dust. *Atmos. Chem. and Phys.* **1–34**. <https://doi.org/10.5194/acp-2021-4> (2021).
74. Bhattachan, A. et al. The Southern Kalahari: A potential new dust source in the Southern Hemisphere? *Environ. Res. Lett.* **7**, 024001 (2012).
75. Bryant, R. G., Bigg, G. R., Mahowald, N. M., Eckardt, F. D. & Ross, S. G. Dust emission response to climate in southern Africa. *J. of Geophys. Res. Atmos.* **112**, D09207 (2007).
76. Todd, M., Washington, R. & Washington, R. Circulation anomalies associated with tropical-temperate troughs in southern Africa and the south west Indian Ocean. *Climate Dynamics* **15**, 937–951 (1999).
77. Gili et al. Isotopic evidence (Sr, Nd and Pb) of South Africa as a dust precursor for atmospheric depositions in Antarctica. in INQUA 1435 (2019).
78. Vanderstraeten et al. Chasing dust in Dronning Maud Land, East Antarctica: a Trace Element perspective. in INQUA 1436 (2019).
79. Vanderstraeten, A. Advances in geochemical tracing of atmospheric dust in Antarctica. (Université libre de Bruxelles, 2020).
80. Li, C. et al. Holocene dynamics of the southern westerly winds over the Indian Ocean inferred from a peat dust deposition record. *Quater. Sci. Rev.* **231**, 1–13 (2020).
81. di Biagio, C. et al. Global scale variability of the mineral dust long-wave refractive index: a new dataset of in situ measurements for climate modeling and remote sensing. *Atmos. Chem. and Phys.* **17**, 1901–1929 (2017).
82. Wang, J. et al. Design of a new multi-phase experimental simulation chamber for atmospheric photosmog, aerosol and cloud chemistry research. *Atmos. Measurement Techniques* **4**, 2465–2494 (2011).
83. Vanderstraeten, A. et al. First multi-isotopic (Pb–Nd–Sr–Zn–Cu–Fe) characterization of dust reference materials (ATD and BCR-723): a multi-column chromatographic method optimised to trace mineral and anthropogenic dust sources. *Geostandards and Geoanal. Res.* **44**, 307–329 (2020).
84. Gingele, F. X. & de Deckker, P. Clay mineral, geochemical and Sr–Nd isotopic fingerprinting of sediments in the Murray–Darling fluvial system, southeast Australia. *Australian J. of Earth Sci.* **52**, 965–974 (2005).
85. Grousset, F. E. & Biscaye, P. E. Tracing dust sources and transport patterns using Sr, Nd and Pb isotopes. *Chemical Geol.* **222**, 149–167 (2005).

## Acknowledgements

This work was supported through Belgian Federal Science Policy Office (BELSPO) fellowship (Convention BR/175/A2/CHASE 1&2). Co-authors would like to warmly thank Jeroen De Jong (ULB) for his assistance during isotopic analyses and the F.R.S-FNRS for the financial support of the analytical platform (e.g. Large Equipments (GEQ) No. 2.5016.12 & 40007934). CNRS-INSU is gratefully acknowledged for supporting CESAM as an open facility through the National Instrument and AERIS datacenter (aeris-data.fr) for hosting simulation chamber data. The CESAM chamber has received funding from the European Union's Horizon 2020 research and innovation program through the EUROCHAMP-2020 Infrastructure Activity under grant agreement No. 730997. Sample collection was supported by the Natural Science and Engineering Research Council of Canada (Discovery Grant RGPIN-2016-05417). All fieldwork conducted in Namibia was supported through permits issued by the Ministry of the Environment and Transport (#2255/2017) and the National Commission on Research, Science, & Technology (#RPV00272018). We gratefully acknowledge the aid of Dr. Hipondoka, Dr. Maggs-Kölling, and the Gobabeb Research and Training Centre in the planning and logistics for the collection of the field samples. We are very grateful for the pertinent comments from von Holdt J. as well as those made by the two other reviewers, who significantly helped to improve and clarify many points of the original manuscript.



### Author contributions

This work was part of S.G. postdoctoral research. S.G. led the writing of the manuscript, analyzed and interpret the geochemical database including the construction of the figures. A.V. helped with the aerosol samples collected with the CESAM simulation chamber and assisted with lab work. A.C. collected the samples as the sampling was part of her Master student's thesis project and was at LISA during the CESAM experiments as a visiting scientist through the MITAC program J.K. contributed to the sampling and the writing of the main text. D.G., B.D., and P.V. contributed to the writing of the discussion and the major revisions. P.F. and C.B. were responsible for our access to the CESAM facilities and helped with the experiments done on the simulation chamber. They also contributed to the writing of the method section. M.C., E.P., and J.F.D. (PI of the CESAM) assisted at the CESAM facilities and N.M. was S.G. PI during her postdoc and therefore the person who supervised and reviewed this project from beginning to end.

### Competing interests

The authors declare no competing interests.

### Additional information

**Supplementary information** The online version contains supplementary material available at <https://doi.org/10.1038/s43247-022-00464-z>.

**Correspondence** and requests for materials should be addressed to Stefania Gili.

**Peer review information** *Communications Earth & Environment* thanks Johanna von Holdt, Akinori Ito and the other, anonymous, reviewer(s) for their contribution to the peer review of this work. Primary Handling Editor: Joe Aslin.

**Reprints and permission information** is available at <http://www.nature.com/reprints>

**Publisher's note** Springer Nature remains neutral with regard to jurisdictional claims in published maps and institutional affiliations.



**Open Access** This article is licensed under a Creative Commons Attribution 4.0 International License, which permits use, sharing, adaptation, distribution and reproduction in any medium or format, as long as you give appropriate credit to the original author(s) and the source, provide a link to the Creative Commons license, and indicate if changes were made. The images or other third party material in this article are included in the article's Creative Commons license, unless indicated otherwise in a credit line to the material. If material is not included in the article's Creative Commons license and your intended use is not permitted by statutory regulation or exceeds the permitted use, you will need to obtain permission directly from the copyright holder. To view a copy of this license, visit <http://creativecommons.org/licenses/by/4.0/>.

© The Author(s) 2022